

# Dosimetric comparison of patient setup strategies in stereotactic body radiation therapy for lung cancer

Jianzhou Wu<sup>a)</sup>

*Radiation Oncology, Swedish Cancer Institute, Seattle, Washington 98104*

Christopher Betzing

*Department of Radiation Medicine, Oregon Health and Science University, Portland, Oregon 97239*

Tongming T. He

*Radiation Oncology, Swedish Cancer Institute, Seattle, Washington 98104*

Martin Fuss

*Department of Radiation Medicine, Oregon Health and Science University, Portland, Oregon 97239*

Warren D. D'Souza

*Department of Radiation Oncology, University of Maryland School of Medicine, Baltimore, Maryland 21044*

(Received 14 January 2013; revised 14 March 2013; accepted for publication 29 March 2013; published 22 April 2013)

**Purpose:** In this work, the authors retrospectively compared the accumulated dose over the treatment course for stereotactic body radiation therapy (SBRT) of lung cancer for three patient setup strategies.

**Methods:** Ten patients who underwent lung SBRT were selected for this study. At each fraction, patients were immobilized using a vacuum cushion and were CT scanned. Treatment plans were performed on the simulation CT. The planning target volume (PTV) was created by adding a 5-mm uniform margin to the internal target volume derived from the 4DCT. All plans were normalized such that 99% of the PTV received 60 Gy. The plan parameters were copied onto the daily CT images for dose recalculation under three setup scenarios: skin marker, bony structure, and soft tissue based alignments. The accumulated dose was calculated by summing the dose at each fraction along the trajectory of a voxel over the treatment course through deformable image registration of each CT with the planning CT. The accumulated doses were analyzed for the comparison of setup accuracy.

**Results:** The tumor volume receiving 60 Gy was  $91.7 \pm 17.9\%$ ,  $74.1 \pm 39.1\%$ , and  $99.6 \pm 1.3\%$  for setup using skin marks, bony structures, and soft tissue, respectively. The isodose line covering 100% of the GTV was  $55.5 \pm 7.1$ ,  $42.1 \pm 16.0$ , and  $64.3 \pm 7.1$  Gy, respectively. The corresponding average biologically effective dose of the tumor was  $237.3 \pm 29.4$ ,  $207.4 \pm 61.2$ , and  $258.3 \pm 17.7$  Gy, respectively. The differences in lung biologically effective dose, mean dose, and V20 between the setup scenarios were insignificant.

**Conclusions:** The authors' results suggest that skin marks and bony structure are insufficient for aligning patients in lung SBRT. Soft tissue based alignment is needed to match the prescribed dose delivered to the tumors. © 2013 American Association of Physicists in Medicine. [<http://dx.doi.org/10.1118/1.4801926>]

Key words: SBRT, IGRT, lung, patient setup, 4D dose calculation

## I. INTRODUCTION

Prior to the availability of in-room image-guidance technology, skin marks were used for patient setup prior to each treatment. However, the interfraction variation of tumor position with respect to the skin marks can lead to large uncertainties in setup.<sup>1,2</sup> The advent of on-board imaging systems has increased the usage of imaging for patient setup.<sup>1-13</sup> Typically, image guided radiation therapy (IGRT) in the form of megavoltage (MV) portal images, orthogonal pairs of kilovoltage (kV) radiographs, or kV/MV cone-beam CT (CBCT) images is used to align patients prior to treatment. Those images are compared with the digitally reconstructed radiographs (DRR) or planning CT images to determine the table shift relative to the treatment planning setup. MV portal images or kV radiographs are useful in the alignment of bony structures or

implanted markers. However, these modalities lack sufficient soft tissue information and hence are not ideal for the alignment of patients with tumors that move with respect to bony structures. CBCT on the other hand has the potential to reveal sufficient soft tissue information for the purposes of patient setup.

IGRT is believed to particularly impact treatment of tumors located in thoracic and abdominal areas, since tumors in these areas are susceptible to respiration induced organ motion. Portal imaging in patient setup for lung cancer reduced setup errors to a few millimeters.<sup>3-6</sup> Similar studies for CBCT based patient setup for lung cancer have also been reported.<sup>1,2,7-13</sup> These investigations concluded that the use of IGRT for patient setup margins used to create the planning target volume (PTV) can be significantly reduced,<sup>1,8,11-13</sup> thereby sparing healthy lung tissue.

For medically inoperable early stage lung cancer, stereotactic body radiation therapy (SBRT) has become an accepted standard treatment modality.<sup>14–21</sup> Due to the curative intent of SBRT for these patients and the already compromised pulmonary function of these patients, accurate targeting while decreasing the margin assumes additional importance. With the introduction of four-dimensional (4D) CT imaging into the clinical workflow, the tumor motion envelop (internal tumor volume or ITV) can be estimated.<sup>22–27</sup> The margin used to create the PTV is 3–5 mm, and is used to account for setup uncertainty.<sup>22–27</sup> The small setup margin used for lung SBRT highlights the importance of accurate patient setup strategies.

Grills *et al.* compared the setup using the tattoos marked on the immobilization devices with that using CBCT, and concluded that setup based on patient immobilization device without image guidance is less optimal.<sup>1</sup> Wang *et al.* compared setup accuracy for lung SBRT using skin marker, orthogonal kV image pair, and CBCT, and concluded that image guidance is useful in order to improve treatment accuracy.<sup>2</sup> The aforementioned studies investigated the table shifts using various setup strategies. However, these studies did not investigate the dosimetric impact of various patient setup strategies. In this study, we retrospectively calculated and compared the accumulated dose over a three-fraction SBRT treatment course when patients were setup using skin marks, bony anatomy, and soft tissue anatomy in an effort to gain insight into the clinical significance of these setup strategies.

## II. METHODS AND MATERIALS

Ten patients who underwent lung SBRT were selected for this study. Each patient was immobilized using a vacuum cushion BodyFIX system (Medical Intelligence, Schwabmuenchen, Germany) and underwent a 4D CT scan and a free-breathing CT scan using a 16-slice big bore CT scanner (Philips Medical Systems, Cleveland, OH). The two scans had identical scan region, image center, and CT coordinates. Following CT scanning, all image sets were imported into the Pinnacle treatment planning system (Philips Medical Systems, Madison, WI). A treatment plan was added, where the free breathing CT image was set as the primary image set, and all the 4D CT images were set as the secondary image sets. All the image sets were intrinsically aligned using the CT coordinates without image registration. The GTV at simulation was contoured on each of the ten 3D CT images corresponding to ten different respiration phases. A uniform 5 mm margin was added to the union of the ten GTVs, the ITV, to generate the PTV. Table I shows the tumor location, volume, and peak-to-peak three-dimensional (3D) tumor motion displacement as measured from the simulation 4D CT for the selected patients. Twelve to fifteen beams were used in the plan depending on tumor location and size. Beam angles were selected such that no entrance beam was allowed to pass through the critical structures, such as cord and heart. About 60 Gy in three fractions was prescribed to cover 99% of the PTV. Free-breathing CT scans were also acquired just prior to each treatment fraction with the patient immobilized in the same

TABLE I. Tumor characteristics of the ten patients used in this study. Tumor radius was calculated by approximating the tumor as a sphere. The last column calculated the ratio of the tumor motion amplitude over the cubic of the tumor radius.

Patient no.	Tumor location	Tumor volume (cm <sup>3</sup> )	3D motion (cm)	Motion/radius <sup>3</sup>
1	LUL	15.1	0.3	0.07
2	RUL	3.3	0.1	0.14
3	RLL	15.2	0.4	0.12
4	LUL	2.0	0.5	1.06
5	RUL	4.0	1.0	1.04
6	RLL	134.0	1.0	0.03
7	RUL	23.1	0.3	0.06
8	RML	3.9	1.0	1.11
9	LLL	9.1	1.2	0.56
10	RLL	20.2	1.7	0.36

Note: LLL = left lower lobe; LUL = left upper lobe; RLL = right lower lobe; RML = right middle lobe; RUL = right upper lobe. Tumor volume was measured at end-exhale.

manner as they were during the simulation procedure and as intended during treatment delivery.

Prior to each treatment, patients were scanned again in their treatment position using an in-room CT scanner, which is identical to the simulation CT scanner. The table of the in-room CT scanner can be aligned and connected to the table of the treatment machine. Patients can be smoothly transferred between the two tables, while retaining the same treatment position within their immobilization cushions. In this study, immediately following the pretreatment scan using the in-room CT scanner, patients were transferred onto the table of the treatment machine. A treatment position verification scan was acquired using the on-board cone-beam CT system (Varian Medical Systems, Palo Alto, CA).

Free-breathing CT images acquired at each fraction were registered to the free-breathing simulation CT in the Pinnacle planning system for the investigation of the dosimetric influence of three patient setup methods, namely, skin-marker based, bony structure based, and soft tissue/tumor based patient setup strategies. First, daily free-breathing CT images were aligned with the planning CT image by matching the skin markers. After skin-marker based initial alignment, an automatic rigid image registration was performed which fused the planning 3D CT to the 3D CT at each treatment using six control parameters: 3D translation along the principle axes and 3D rotation around these axes. Normalized mutual information was used as the cost function to register the images. A registration clip box was used to minimize the influence of voxels located far away from the tumor on the outcome of the image registration. The clip box was defined on the planning CT image and roughly contained the patient's body contour in the axial plane and extended about 2–3 cm beyond the extreme positions of the PTV in the superior–inferior direction. Following rigid registration, the matching of the vertebrae was carefully reviewed. If necessary, minor adjustments were performed to further improve the alignment of the vertebrae. After the alignment of the vertebrae, tumor boundaries

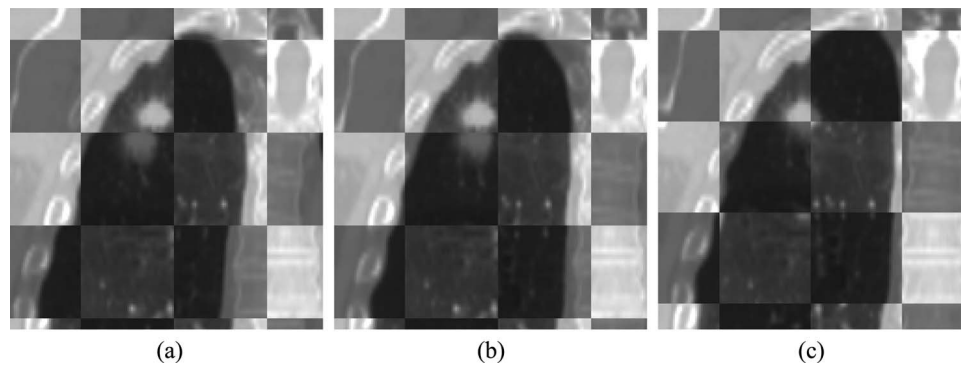


FIG. 1. Coronal view of the alignment of the CT scan on fraction one (dark image) with respect to the planning CT (bright image) for a representative patient. (a) Alignment based on the match of external markers; (b) alignment based on the match of bony structures; and (c) alignment based on the match of soft tissues.

were aligned manually between the planning CT images and the CT images acquired on the day of treatment (with the patient in the same immobilization) for soft tissue alignment.

For each setup scenario, the net 3D shifts between the CT images acquired prior to each treatment fraction and the planning CT images were calculated. The net shifts were applied to the planning isocenter in order to determine the isocenter coordinates on the CT images acquired at each fraction. The tumor centroid on the CT at each treatment was treated as the reference, and the coordinate differences between the isocenters determined from each setup scenario were calculated.

To recalculate the dose received by tissues at each treatment fraction, we copied the plan parameters from the treatment plan corresponding to the planning CT onto the CT acquired just prior to each treatment fraction with the transformed isocenter that simulated the net shifts determined from each of the setup scenarios. The dose for each treatment fraction was recalculated and the monitor units (MUs) corresponding to each beam were forced to those in the original plan.

In order to calculate the accumulated dose over the whole treatment course, we first registered the CT from each fraction to the simulation CT using B-Spline based deformable registration algorithm (ITK). The registration accuracy of this software package has been extensively studied.<sup>28-31</sup> The resultant registration field provided the trajectory of voxel transformation between CT images acquired prior to each fraction. The recalculated dose at each fraction was summed along voxel transformations derived from the deformable registration to generate the accumulated dose to the patient anatomy. The accumulated doses to the GTV and to the total lung were compared using the following parameters: biologically effective dose (BED), normalized total dose delivered in 2 Gy/fraction (NTD), percent volume receiving at least 60 Gy (V60), and minimum dose received by 100% of the GTV (D100). For lung dose analysis, BED, NTD, V20, and mean lung dose (MLD) were compared. The BED and NTD were defined as  $BED = \text{total dose} \times (1 + d/(\alpha/\beta))$ ,  $NTD = BED/(1 + 2Gy/(\alpha/\beta))$ , where  $d = \text{local dose per fraction}$ . In this work, we assumed  $\alpha/\beta = 10$  Gy for tumor and 3 Gy for normal lung.

### III. RESULTS

Figure 1 shows the checker board view of the alignment of a representative patient using three setup strategies investigated in this work. The dark image is the CT scan immediately prior to the first fraction and the bright image is the planning CT scan used for treatment planning. The match of the skin marks on both CT images [Fig. 1(a)] in this case not only misaligned the bony structures but also the tumor. The match of the vertebrae [Fig. 1(b)] improved patient setup. However, a substantial part of the tumor was still misaligned. The match in soft tissues [Fig. 1(c)] accurately aligned the tumor but with some degree of misalignment with respect to vertebrae.

Table II lists the absolute offsets of the treatment isocenters with respect to the tumor centroids for each patient setup strategy averaged over the 30 alignments for the ten patients. Bony structure-based patient setup did not improve alignment accuracy compared with skin mark-based patient setup strategy. The average alignment error of the skin mark-based strategy was less than 5 mm (margin used to create the PTV). However, the average alignment error using the vertebrae exceeded 5 mm. The largest alignment error occurred in the superior-inferior direction. The soft tissue based patient setup strategy had the lowest average alignment errors (well within the uniform margin used to create the PTV).

Figure 2 shows the isodose coverage of the accumulated dose on the planning CT using the three setup strategies. The thick black curve is the GTV, the thin gray curves correspond to the 100%, 90%, 50%, and 25% isodose lines, respectively (100% = 60 Gy). For patient setup using external markers and vertebrae structures, an assessment of the accumulated dose shows that it would underdose the tumor. Figure 3 shows the

TABLE II. Absolute offsets (mm) of the treatment isocenters with respect to the tumor geometric center for each patient setup strategy averaged over the 30 alignments for the ten patients.

	Marker/tattoo	Bony structure	Soft tissue
Lateral (mm)	$4.0 \pm 3.0$	$6.6 \pm 4.6$	$2.1 \pm 1.7$
Anterior-posterior (mm)	$3.2 \pm 2.1$	$5.9 \pm 3.2$	$2.0 \pm 1.9$
Superior-inferior (mm)	$4.8 \pm 4.2$	$8.8 \pm 7.1$	$2.2 \pm 2.0$

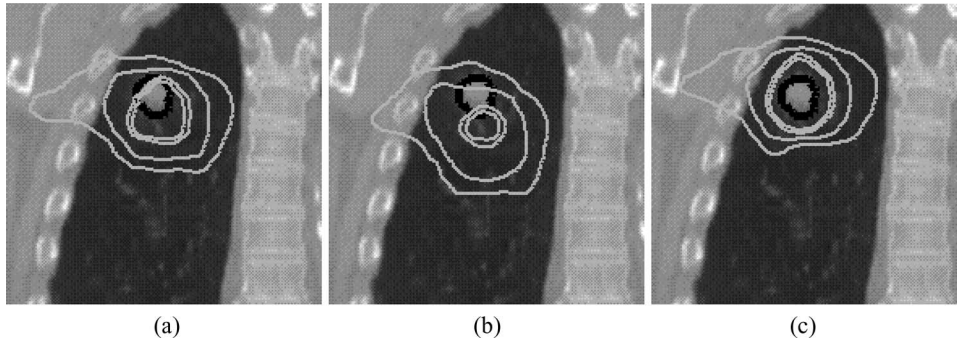


FIG. 2. Isodose distribution of the accumulated total dose (three fractions) shown on the planning CT with the assumption that patient setup was based on the matching of (a) external markers, (b) vertebrae, and (c) soft tissues. The thick black curve is the GTV, the thin gray curves correspond to the 100%, 90%, 50%, and 25% isodose lines, respectively (100% = 60 Gy).

dose volume histogram (DVH) of the accumulated dose for this representative patient. The dotted, dashed, and solid lines correspond to DVHs for patient setup based on the matching of external markers, bony structures, and soft tissues, respectively. The accumulated dose was estimated on the planning CT.

Figure 4 shows the accumulated tumor V60 and D100 for the ten patients for the three patient setup scenarios. For the

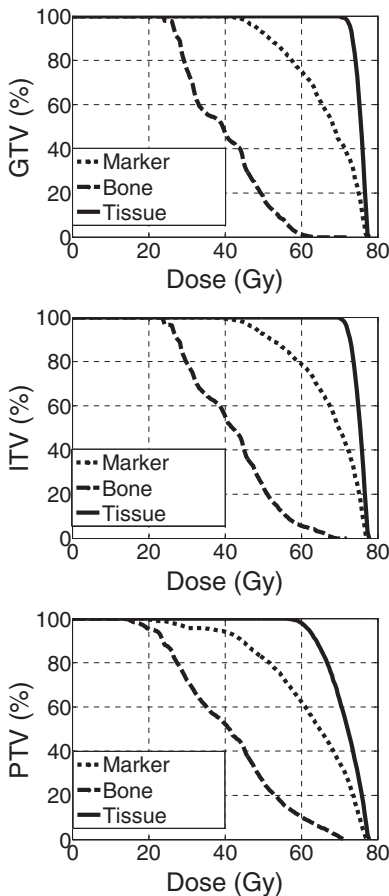


FIG. 3. Dose volume histograms of the accumulated dose for the representative patient after finishing the treatment course (three fractions). The dotted, dashed, and solid lines correspond to patient setup based on the matching of external markers, bony structures, and soft tissues, respectively.

two cases (cases 4 and 5) where the tumors are small and motions are relative large, as shown in Table I, vertebrae-based patient setup would lead to severe geometric misses of the tumors. The resultant tumors V60 and D100 are very small. Tables III and IV list the mean V60 and mean D100 of the ITV and PTV averaged over the ten patients for the three setup scenarios.

Figure 5 shows the mean and standard deviation of the tumor V60, D100, BED, and NTD averaged over the ten patients corresponding to the three setup strategies. The tumor V60 was  $91.7 \pm 17.9$ ,  $74.1 \pm 39.1$ , and  $99.6 \pm 1.3\%$  for patient setup using external markers, bony structures, and soft tissue, respectively. The isodose line covering 100% of the GTV (D100) was  $55.5 \pm 7.1$ ,  $42.1 \pm 16.0$ , and  $64.3 \pm 7.1$  Gy for the three setup strategies, respectively. Similarly, the

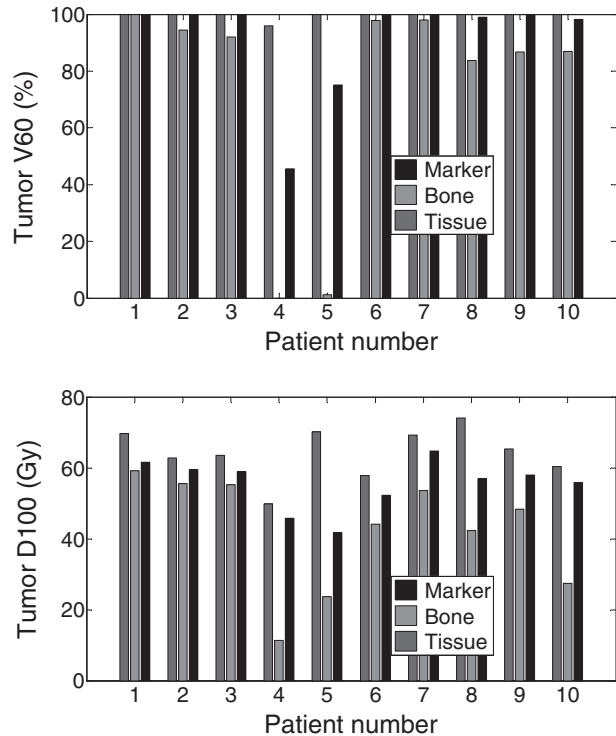


FIG. 4. Tumor V60 (%) and D100 (Gy) for the ten patients with patient setup using external markers, bony structures, and soft tissue.

TABLE III. The mean V60 (%) and mean D100 (Gy) of the ITV averaged over the ten patients for patient setup using external markers, bony structures, and soft tissue.

	Marker/tattoo	Bony structure	Soft tissue
V60 (%)	92.7 ± 8.4	70.1 ± 35.6	98.8 ± 2.6
D100 (Gy)	46.9 ± 9.7	33.3 ± 15.1	58.3 ± 8.2

isodose line covering 100% of ITV was  $46.9 \pm 9.7$ ,  $33.3 \pm 15.1$ , and  $58.3 \pm 8.2$  Gy, and covering 95% of the PTV was  $43.2 \pm 10.6$ ,  $30.8 \pm 13.4$ , and  $53.6 \pm 6.8$  Gy, respectively. The above results show improved results when the tumor soft tissue was used for alignment. Tumor BED averaged over the ten patients was  $237.3 \pm 29.4$ ,  $207.4 \pm 61.2$ , and  $258.3 \pm 17.7$  Gy for patient setup using external markers, bony structures, and soft tissue, respectively. The corresponding tumor NTD was  $205.9 \pm 16.9$ ,  $172.8 \pm 51.0$ , and  $215.3 \pm 14.7$ , respectively. The Student's *t*-test showed that the difference in tumor V60, D100, BED, and NTD between external marker based or bony structure based alignment and soft tissue based alignment was significant ( $p < 0.05$ ).

Figure 6 shows the mean and standard deviation of the BED, NTD, MLD, and V20 (percent volume received at least 20 Gy) of the total lung averaged over the ten patients corresponding to the three setup strategies. The mean BED was  $9.4 \pm 3.8$ ,  $9.2 \pm 3.6$ , and  $9.4 \pm 3.0$  Gy for patient setup using external markers, bony structures, and soft tissue, respectively. The corresponding NTD was  $7.9 \pm 3.1$ ,  $7.7 \pm 3.0$ , and  $7.8 \pm 3.8$  Gy, respectively. The MLD was  $4.9 \pm 1.9$ ,  $4.9 \pm 1.8$ , and  $4.9 \pm 2.0$  Gy, lung V20 was  $6.4 \pm 2.3$ ,  $6.3 \pm 2.2$ , and  $6.5 \pm 2.5\%$  for patient setup using external markers, bony structures, and soft tissue, respectively. The difference in total lung BED, NTD, MLD, and V20 among these three setup strategies was insignificant ( $p > 0.5$ ).

#### IV. DISCUSSION

This study investigated the influence of three patient setup strategies on the accumulated dose received by the patient for lung SBRT. 4D CT images were used to define the ITV and a uniform margin of 5 mm was used to create the PTV. The results from our study show that even though patients were immobilized with a vacuum cushion, patient setup by matching skin marks or vertebrae may not result in acceptable tumor dose coverage. Therefore, treatments with patient setup based on either skin marks or bony structures would underdose the tumor. Only soft-tissue based setup results in setup errors of

TABLE IV. The mean V60 (%) of the PTV and mean D100 (Gy) to the 95% PTV averaged over the ten patients for patient setup using external markers, bony structures, and soft tissue.

	Marker/tattoo	Bony structure	Soft tissue
V60 (%)	74.8 ± 13.3	55.3 ± 26.3	87.4 ± 7.9
D100 (Gy)	43.2 ± 10.6	30.8 ± 13.4	53.6 ± 6.8

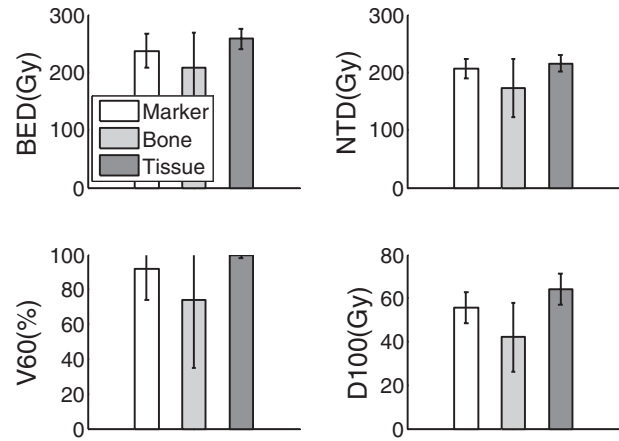


FIG. 5. Mean and standard deviation of the tumor BED, NTD, V60, and D100 averaged over the ten patients corresponding to the external marker, bony structure, and soft tissue-based setup.

less than 5 mm, a margin that we used for the PTV generation to ensure adequate dose coverage to the GTV. By contrast, the influence of patient setup strategies on total lung dose is minimal. We attribute this minimal effect on lung dose to the small tumor volumes in lung SBRT cases. The limitation dose to the critical structures, such as cord and heart, is sensitive to the image registrations. In this study, patients had peripheral tumors. During treatment planning, beam angles were selected such that the maximum doses to the critical structures were very low as compared with the limitation doses. The impact of image registrations to the maximum doses of the critical structures was minimal in the study.

Our study shows that for most of the cases, tumor dose coverage corresponding to vertebrae-based patient setup results in poorer dose coverage compared with the skin mark-based setup strategy. In our clinic, skin markers are normally placed on or close to the CT slices where the tumors are present. Therefore, matching of the skin markers leads to a coarse matching of local anatomy surrounding the tumor. In contrast, vertebrae-based setup parameters were obtained through 3D

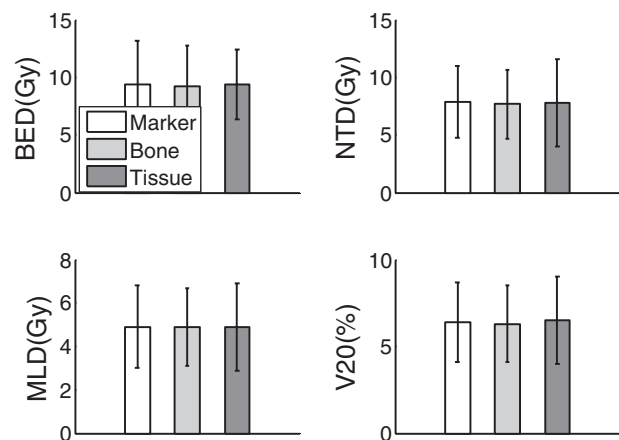


FIG. 6. Mean and standard deviation of the lung BED, NTD, mean dose, and V20 of the total lung averaged over the ten patients corresponding to the external marker, bony structure, and soft tissue-based setup.

rigid registration performed within a clip box. In our clinic, this registration box is normally designed so that it extends 2 cm or more in the superior–inferior direction beyond the extremities of the PTV. Image matching was performed using the CT information within the whole clip box. Hence, for vertebrae-based setup, local matching accuracy was compromised to yield a better global matching. This degradation of local matching accuracy happens when the daily vertebrae curvature does not match well with that on the treatment planning CT, or when there are rotations of the daily CT images around the principle axes with respect to the treatment planning CT. Our treatment table cannot correct pitch and roll. Therefore, matching of bony structure without rotation correction may lead to degradation of local alignment accuracy. Nevertheless, tumor-tissue-based alignment is likely to result in improved tumor coverage compared with other setup strategies.

This study also shows that the accuracy of patient setup in terms of tumor dose coverage is dependent on both the tumor size and the tumor displacement. For small tumors with large displacement, bony structure based setup has a higher possibility of misalignment of the tumor, resulting in underdosing of the tumor. On the other hand, for big tumors with small displacement, underdosing of the tumor is less likely. When the ratio of the tumor motion to the cube of tumor radius (the shape of tumors was approximated as a sphere) is greater than 0.5, vertebrae-based patient setup resulted in underdosing of the tumor.

Our results on the absolute offsets of the treatment isocenters with respect to the tumor geometric center for various setup strategies are consistent with those reported in the literature.<sup>2,7,10</sup> Wang *et al.* reported that correction of patient alignment using CBCT after the initial setup using orthogonal portal images could be more than 1 cm, even though the mean correction was about 2 mm.<sup>2</sup> Guckenberger *et al.* showed that patient setup using bony structure may not be able to accurately align the tumor.<sup>7</sup> These reports concluded that bony structure based patient setup may not agree with soft tissue based setup with discrepancies greater than 5 mm.

This study focused on calculating the accumulated dose distribution for three setup strategies. Our result confirmed from dosimetric point of view that bony structure based patient setup strategy may lead to underdosing of the tumor and only soft tissue based setup can reliably deliver the intended dose to the tumor. Determination of margin size used to create the PTV should be carefully considered and depends on the selection of patient setup strategies. For patient setup using orthogonal portal film pairs, normally a large margin (8–10 mm) in the superior–inferior direction should be used to account for setup uncertainty.<sup>32</sup> While for patient setup using CBCT, usually a tight 3–5 mm margin is applied uniformly.<sup>22–27</sup> Patient immobilization devices are also frequently used to reduce patient setup uncertainty,<sup>1,2,7,23</sup> hence reducing the margin used to create the PTV. However, our results show that even though immobilization was used in our study, skin marker and bony structure-based alignment were still not sufficient to ensure adequate tumor coverage if a uniform 5 mm margin was used to create the PTV.

Several factors account for the degradation of tumor dose coverage, such as patient setup uncertainty, respiration induced tumor motion, changes in breathing pattern, errors introduced by image registrations, etc. In this study, we separated the impact of patient setup uncertainty from the impacts of all other factors. We investigated how seriously the setup uncertainty would impact the dose coverage. We recalculated the fractional doses on the free breathing CT images, which intrinsically neglected the impact of interfractional and intrafractional respiration induced tumor motion. We also assumed that the image registrations introduced no additional uncertainty. There are studies in literature that investigated how respiration would impact tumor dose coverage.<sup>33,34</sup> In a separate study, we investigated how the changes in breathing pattern affected tumor dose coverage.<sup>35</sup>

It has been shown that CBCT delivers non-negligible dose to the patient.<sup>36,37</sup> Therefore, setup using kV images may be preferred to the setup using CBCT. Lung SBRT treatments normally involve 3–5 fractions, the dose associated with image guidance is a small fraction of the therapeutic dose. The tradeoff between additional dose delivered by CBCT scanning and margin size used to create the PTV should be considered.

## V. CONCLUSIONS

Our results suggest that for SBRT of lung cancer, skin mark and bony structure-based patient setups lead to underdosing of the tumor and, hence, are inaccurate for aligning patients. Soft tissue (derived from conventional CT, CBCT) based alignment is necessary to match the planned dose to the tumors. On the other hand, the difference in lung dose among these three alignment strategies considered in this work is indistinguishable.

## ACKNOWLEDGMENT

The authors report no conflicts of interest in conducting the research.

<sup>a</sup>Author to whom correspondence should be addressed. Electronic mail: jianzhou.wu@Swedish.org; Telephone: (425)313-4214; Fax: (425)313-4201.

<sup>1</sup>I. S. Grills *et al.*, “Image-guided radiotherapy via daily online cone-beam CT substantially reduces margin requirements for stereotactic lung radiotherapy,” *Int. J. Radiat. Oncol., Biol., Phys.* **70**, 1045–1056 (2008).

<sup>2</sup>Z. Wang *et al.*, “Refinement of treatment setup and target localization accuracy using three-dimensional cone-beam computed tomography for stereotactic body radiotherapy,” *Int. J. Radiat. Oncol., Biol., Phys.* **73**, 571–577 (2009).

<sup>3</sup>H. C. de Boer *et al.*, “Analysis and reduction of 3D systematic and random setup errors during the simulation and treatment of lung cancer patients with CT-based external beam radiotherapy dose planning,” *Int. J. Radiat. Oncol., Biol., Phys.* **49**, 857–868 (2001).

<sup>4</sup>S. C. Erridge *et al.*, “Portal imaging to assess set-up errors, tumor motion and tumor shrinkage during conformal radiotherapy of non-small cell lung cancer,” *Radiother. Oncol.* **66**, 75–85 (2003).

<sup>5</sup>J. R. Van Sornsen *et al.*, “Procedures for high precision setup verification and correction of lung cancer patients using CT-simulation and digitally reconstructed radiographs (DRR),” *Int. J. Radiat. Oncol., Biol., Phys.* **55**, 804–810 (2003).

- <sup>6</sup>R. I. Berbeco *et al.*, "Clinical feasibility of using an EPID in CINE mode for image-guided verification of stereotactic body radiotherapy," *Int. J. Radiat. Oncol., Biol., Phys.* **69**, 258–266 (2007).
- <sup>7</sup>M. Guckenberger *et al.*, "Cone-beam CT image-guidance for extra-cranial stereotactic radiotherapy of intrapulmonary tumors," *Acta. Oncol.* **45**, 897–906 (2006).
- <sup>8</sup>L. Wang *et al.*, "Benefit of three-dimensional image-guided stereotactic localization in the hypofractionated treatment of lung cancer," *Int. J. Radiat. Oncol., Biol., Phys.* **66**, 738–747 (2006).
- <sup>9</sup>G. R. Borst *et al.*, "Kilo-voltage cone-beam computed tomography setup measurements for lung cancer patients: First clinical results and comparison with electronic portal-imaging device," *Int. J. Radiat. Oncol., Biol., Phys.* **68**, 555–561 (2007).
- <sup>10</sup>T. G. Purdie *et al.*, "Cone-beam computed tomography for on-line guidance of lung stereotactic radiotherapy: Localization, verification, intrafraction tumor position," *Int. J. Radiat. Oncol., Biol., Phys.* **68**, 243–252 (2007).
- <sup>11</sup>J. P. Bissonnette *et al.*, "Cone-beam computed tomographic image guidance for lung cancer radiation therapy," *Int. J. Radiat. Oncol., Biol., Phys.* **73**, 927–934 (2009).
- <sup>12</sup>A. R. Yeung *et al.*, "Tumor localization using cone-beam CT reduces setup margins in conventionally fractionated radiotherapy for lung tumors," *Int. J. Radiat. Oncol., Biol., Phys.* **74**, 1100–1107 (2009).
- <sup>13</sup>J. Zhou *et al.*, "Analysis of daily setup variation with tomotherapy megavoltage computed tomography," *Med. Dosim.* **35**, 31–37 (2010).
- <sup>14</sup>M. Uematsu *et al.*, "Focal, high dose, and fractionated modified stereotactic radiation therapy for lung carcinoma patients: A preliminary experience," *Cancer* **82**, 1062–1070 (1998).
- <sup>15</sup>R. Timmerman *et al.*, "Extracranial stereotactic radioablation: Results of a phase I study in medically inoperable Stage I non-small cell lung cancer," *Chest* **124**, 1946–1955 (2003).
- <sup>16</sup>H. Hof *et al.*, "Stereotactic single-dose radiotherapy of Stage I non-small cell lung cancer (NSCLC)," *Int. J. Radiat. Oncol., Biol., Phys.* **56**, 335–341 (2003).
- <sup>17</sup>R. I. Whyte *et al.*, "Stereotactic radiosurgery for lung tumors: Preliminary report of a phase I trial," *Ann. Thorac. Surg.* **75**, 1097–1101 (2003).
- <sup>18</sup>H. Onishi *et al.*, "Clinical outcomes of stereotactic radiotherapy for Stage I non-small cell lung cancer using a novel irradiation technique: Patient self-controlled breath-hold and beam switching using a combination of linear accelerator and CT scanner," *Lung Cancer* **45**, 45–55 (2004).
- <sup>19</sup>J. Wulf *et al.*, "Stereotactic radiotherapy for primary lung cancer and pulmonary metastases: A noninvasive treatment approach in medically inoperable patients," *Int. J. Radiat. Oncol., Biol., Phys.* **60**, 186–196 (2004).
- <sup>20</sup>T. Xia *et al.*, "Promising clinical outcome of stereotactic body radiation therapy for patients with inoperable Stage I/II non-small-cell lung cancer," *Int. J. Radiat. Oncol., Biol., Phys.* **66**, 117–125 (2006).
- <sup>21</sup>M. Hiraoka, Y. Matsuo, and Y. Nagata, "Stereotactic body radiation therapy (SBRT) for early-stage lung cancer," *Cancer Radiother.* **11**, 32–35 (2007).
- <sup>22</sup>W. D. D'Souza *et al.*, "The use of gated and 4D CT imaging in planning for stereotactic body radiation therapy," *Med. Dosim.* **32**, 92–101 (2007).
- <sup>23</sup>J. Wu *et al.*, "An evaluation of planning techniques for stereotactic body radiation therapy in lung tumors," *Radiother. Oncol.* **87**, 35–43 (2008).
- <sup>24</sup>A. Richter *et al.*, "Influence of increased target dose inhomogeneity on margins for breathing motion compensation in conformal stereotactic body radiotherapy," *BMC Med. Phys.* **8**, 5 (2008).
- <sup>25</sup>H. Hof *et al.*, "4D-CT-based target volume definition in stereotactic radiotherapy of lung tumours: Comparison with a conventional technique using individual margins," *Radiother. Oncol.* **93**, 419–423 (2009).
- <sup>26</sup>L. Wang *et al.*, "Dosimetric comparison of stereotactic body radiotherapy using 4D CT and multiphase CT images for treatment planning of lung cancer: Evaluation of the impact on daily dose coverage," *Radiother. Oncol.* **91**, 314–324 (2009).
- <sup>27</sup>B. Zhao *et al.*, "Image-guided respiratory-gated lung stereotactic body radiotherapy: Which target definition is optimal?," *Med. Phys.* **36**, 2248–2257 (2009).
- <sup>28</sup>T. Popa *et al.*, "ITK implementation of deformable registration methods for time-varying (4D) imaging data," *Proc. SPIE* **6141**, 750–759 (2006).
- <sup>29</sup>V. Noblet *et al.*, "Retrospective evaluation of a topology preserving non-rigid registration method," *Med. Image Anal.* **10**, 366–384 (2006).
- <sup>30</sup>P. A. Andres and R. A. Isoardi, "Using ITK platform for medical image registration," *J. Phys.: Conf. Ser.* **90**, 012056 (2007).
- <sup>31</sup>H. Zhong, J. Kim, and I. J. Chetty, "Analysis of deformable image registration accuracy using computational modeling," *Med. Phys.* **37**, 970–979 (2010).
- <sup>32</sup>Y. Nagata *et al.*, "Clinical outcomes of 3D conformal hypofractionated single high-dose radiotherapy for one or two lung tumors using a stereotactic body frame," *Int. J. Radiat. Oncol., Biol., Phys.* **52**, 1041–1046 (2002).
- <sup>33</sup>M. A. Admiraal, D. Schuring, and C. W. Hurkmans, "Dose calculations accounting for breathing motion in stereotactic lung radiotherapy based on 4D-CT and the internal target volume," *Radiother. Oncol.* **86**, 55–60 (2008).
- <sup>34</sup>H. Kang *et al.*, "Evaluation of tumor motion effects on dose distribution for hypofractionated intensity-modulated radiotherapy of non-small-cell lung cancer," *J. Appl. Clin. Med. Phys.* **11**(3), 78–89 (2010).
- <sup>35</sup>J. Wu *et al.*, "Impact of interfractional tumor motion on respiratory gated stereotactic body radiation therapy for lung tumors," *Med. Phys.* **39**, 3909 (2012).
- <sup>36</sup>L. C. Peng *et al.*, "Dose comparison of megavoltage cone-beam and orthogonal-pair portal images," *J. Appl. Clin. Med. Phys.* **8**(1), 10–20 (2007).
- <sup>37</sup>G. X. Ding, D. M. Duggan, and C. W. Coffey, "Accurate patient dosimetry of kilovoltage cone-beam CT in radiation therapy," *Med. Phys.* **35**, 1135–1144 (2008).